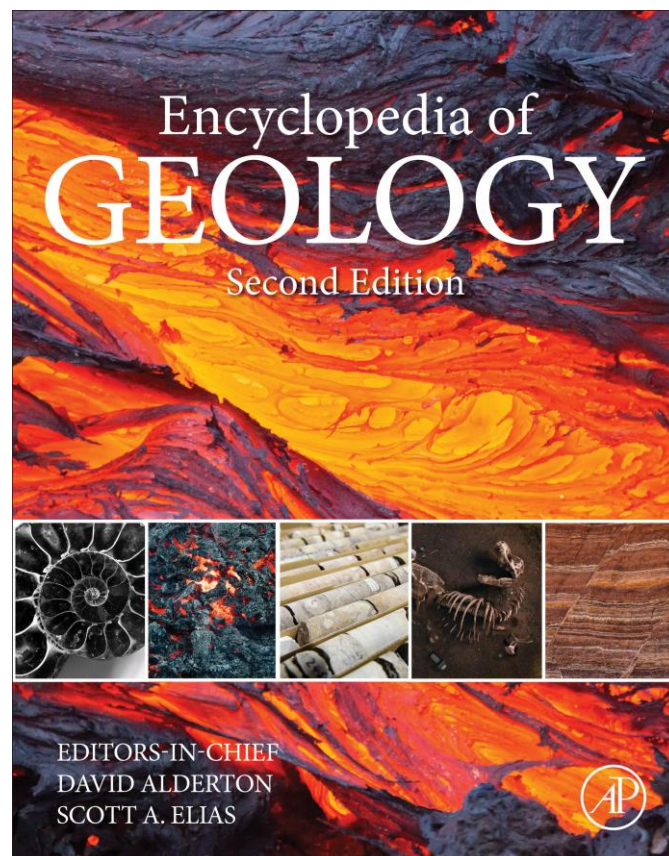


Provided for non-commercial research and educational use.
Not for reproduction, distribution or commercial use.

This article was originally published in *Encyclopedia of Geology*, second edition published by Elsevier, and the attached copy is provided by Elsevier for the author's benefit and for the benefit of the author's institution, for non-commercial research and educational use, including without limitation, use in instruction at your institution, sending it to specific colleagues who you know, and providing a copy to your institution's administrator.



All other uses, reproduction and distribution, including without limitation, commercial reprints, selling or licensing copies or access, or posting on open internet sites, your personal or institution's website or repository, are prohibited. For exceptions, permission may be sought for such use through Elsevier's permissions site at:

<https://www.elsevier.com/about/policies/copyright/permissions>

Sen Gautam, and Stern Robert J. (2021) Subduction Zone Magmas. In: Alderton, David; Elias, Scott A. (eds.) *Encyclopedia of Geology*, 2nd edition. vol. 2, pp. 33-51. United Kingdom: Academic Press.

dx.doi.org/10.1016/B978-0-08-102908-4.00086-2

© 2021 Elsevier Ltd. All rights reserved.

Subduction Zone Magmas

Gautam Sen^a, Lehman College, Bronx, NY, United States

Robert J Stern, University of Texas at Dallas, Richardson, TX, United States

© 2021 Elsevier Ltd. All rights reserved.

Introduction	33
Magmatism in Arcs	37
Lavas	37
Phenocryst Mineralogy	39
Trace Element Composition	39
Isotope Composition	40
Large Ignimbrite Eruptions: The Long Valley Caldera Example	40
Composition of Precaldera, Bishop Tuff, and Postcaldera Lavas	41
Plutons	43
Sierra Nevada Batholith (SNB)	43
Primary Magmas and Daly Gap	44
Fluid-Fluxed Melting in the Asthenospheric Wedge: Insights From Experimental Petrology	48
Fluid Production	49
Melting and Melt Composition	49
Summary of Experimental Petrology Results	51
References	51

Glossary

Critical point A point on a phase diagram at which both the liquid and gas phases of a substance have the same density, and are therefore indistinguishable. The transition between a low-density liquid water and a high-density liquid terminates at P and T significantly greater than the liquid-gas critical point and is called the second critical point.

Fractional crystallization The removal of minerals from a melt, changing the composition of magma from mafic to felsic with time. In most cases, fractional crystallization is the removal of early formed crystals from an originally homogeneous magma (e.g., by gravity settling) so that these crystals are prevented from further reaction with the residual melt.

Liquidus, solidus Refers to thermodynamic phase diagrams showing the equilibrium phases (i.e., melt vs. different kinds of crystals) present as a function of temperature (T), pressure (P), and composition (x). Liquidus surface describes the T-P-x environment where melt is in equilibrium with trace minerals; at higher T only melt exists. Solidus describes the T-P-x environment where minerals are in equilibrium with trace melt; at lower T only solid exists.

Magma chamber A magma chamber is a large pool of melt beneath the surface of the Earth, generally 1–10 km beneath the surface. Many volcanoes are situated over magma chambers. A wide range of processes go on in magma chambers, including assimilation of surrounding crust and fractional crystallization.

Parent magma, primitive magma Melts in equilibrium with mantle minerals. Primitive magmas are rich in Mg and Ni; they undergo complex processes in magma chambers to yield evolved magmas rich in Si and poor in Mg and Ni.

Pyroclastic and Volcaniclastic Pyroclastic rocks or pyroclastics (derived from Greek words for “fire” and “broken”) are sedimentary clastic rocks composed solely or primarily of volcanic materials. Many pyroclastic rocks are deposited by violent eruptions. Where the volcanic material has been transported and reworked through mechanical action, such as by wind or water, these rocks are termed volcaniclastic.

Introduction

Subduction zones are regions of lithospheric downwelling associated with convergent plate margins. They are defined with earthquakes triggered by the recycling of oceanic lithosphere (Fig. 1) and lie beneath important regions of igneous activity. Regions of subduction-related igneous activity are often referred to as island arcs or continental arcs, depending on whether the underlying crust is oceanic (thin) or continental (thick). The Lesser Antilles island arc is a good example, which formed due to the subduction of Atlantic oceanic lithosphere beneath the Caribbean plate. Continental arcs form where an oceanic plate subducts beneath a continental margin. The volcanic front of the Andes Mountains of South America is an example of this.

^aDeceased.

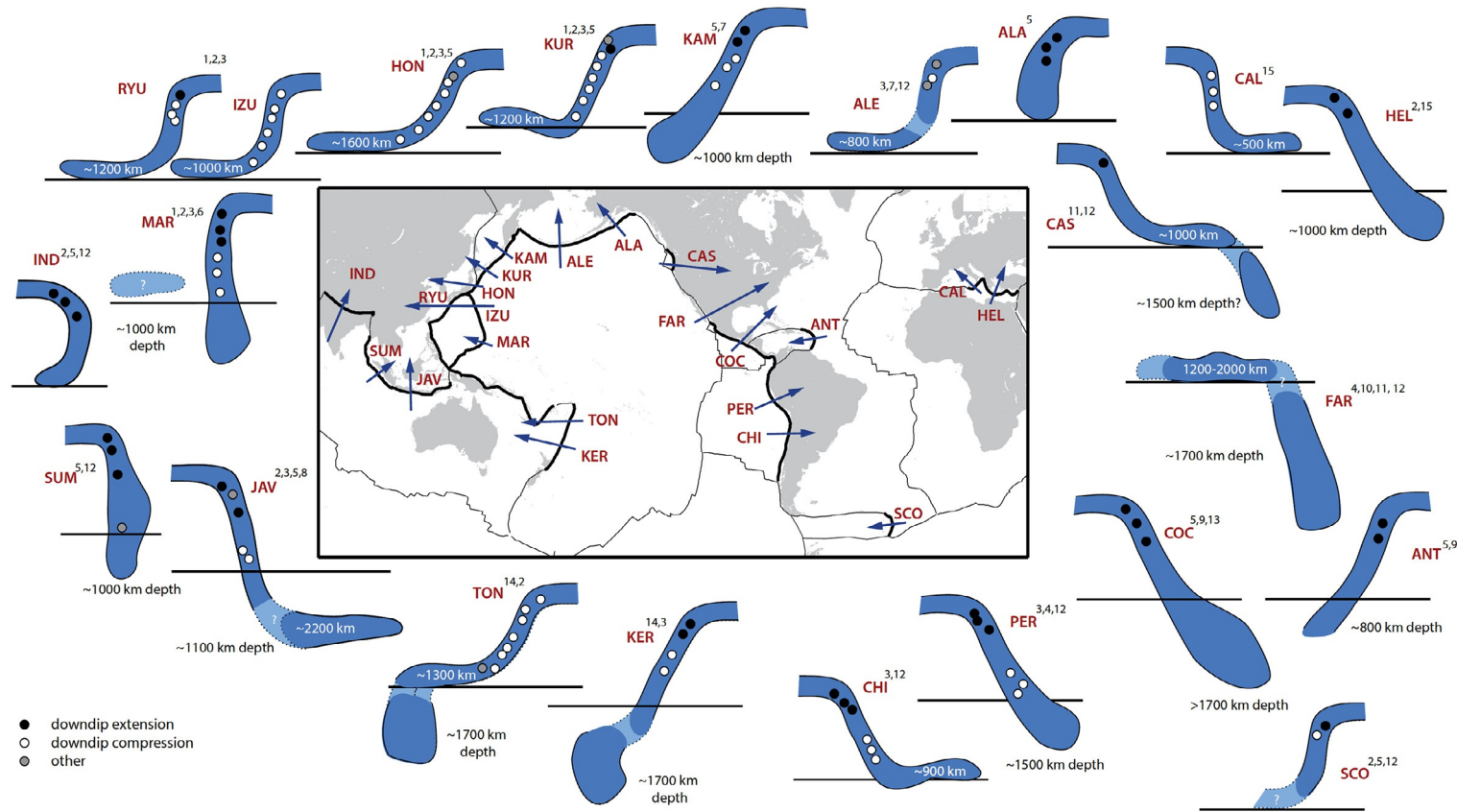


Fig. 1 Map in the center shows active convergent plate boundaries where subduction is occurring. The arrows indicate the direction of dip of the subducting plate. ALA: Alaska, ALE: Aleutian, CAS: Cascadia, FAR: Farallon, COC: Cocos, ANT: Antilles, PER: Peru, CHI: Chile, SCO: Scotia, CAL: Calabria, HEL: Hellenic, IND: India, SUM: Sumatra, JAV: Java, MAR: Marianas, IZU: Izu, HON: Honshu, RYU: Ryukyu, KUR: Kurile, KAM: Kamchatka, TON: Tonga, KER: Kermadec. Goes S, Agrusta R, van Hunen J, and Garel F (2017) Subduction-transition zone interaction: A review. *Geosphere* 13: 644.

An animation showing how oceanic lithosphere is created at mid-ocean ridges and how subduction zones operate can be viewed at <https://www.youtube.com/watch?v=6wJB0k9xjto>.

Subduction zones are the deep expressions of a convergent plate margin. The convergent margin itself can be subdivided along strike into forearcs, magmatic arcs, and back arc regions. This entry is particularly focused on arc igneous activity. This occurs only at sites where the subducting plate's dip is greater than 25 degrees. The average dip of subducting slabs is about 45 degrees at shallow depths (to ~200 km); however, as Fig. 1 shows, this dip can change considerably as a slab descends to greater depths. One constant feature of subduction zones is that the volcanic front occurs 80–130 km above the dipping seismic zone (known as the Wadati-Benioff zone after the Japanese and American scientists who first described these) regardless of the dip of the subducting plate.

There is great variation in physical and magmatic characteristics of subduction zones. In some cases, where the subducting slab is very old and cold, it plunges to the great depths of the lower mantle, which begins 660 km beneath Earth's surface (e.g., Sumatra, Java, and Marianas; Fig. 1). In other cases, the descending slab cannot penetrate the 660 km discontinuity and hugs the bottom of the Transition Zone (e.g., Izu, Honshu, Aleutians). In addition to changing dip along their descent path, most subducted slabs “roll back,” causing the trench and subducted slab to migrate toward the ocean.

In understanding the great variability of subduction zones and associated magmatism, one can look at circum-Pacific subduction zones as a starting point. The eastern margin of the Pacific Ocean is marked by continental magmatic arcs, which developed due to subduction of oceanic lithosphere beneath continental lithosphere. Chilean magmatism is an example of this, where a young (5–10 Ma) and hot Nazca plate is subducted at a shallow angle beneath Chile (Fig. 2). On the other side, the western Pacific is marked by many island arcs that formed due to oceanic-oceanic convergence. A good example is the Izu-Bonin-Marianas (IBM) arc, south of Japan, where cold, dense, 150 Ma (older at greater depths) lithosphere is being subducted at a steep angle beneath another oceanic plate. This type of subduction creates back-arc extension, where decompression melting generates basaltic magmas (Fig. 2).

Andesites are the most diagnostic magma type erupted in arcs, although basalts are more abundant in island arcs. Additionally, rhyolite volcanoes and granitoid plutons are common in continental arcs.

Notwithstanding the great variability of arc igneous activity and seismicity associated with subduction zones, we can start with some general features of subduction related igneous activity. A typical schematic cross-section through an island arc is shown in Fig. 3A (after Stern, 2002). A deep trench marks where the oceanic plate begins to sink beneath the overriding plate. Most trenches associated with island arcs are sediment-starved whereas trenches next to continental arcs often have an abundance of sediments, which are a mix of marine and continentally derived detritus. In fore-arcs with high sediment flux, enormous packages of sediments are deformed to produce an “accretionary wedge” or “accretionary prism” (Fig. 3B). Fragments of the fore-arc crust and mantle may get sliced up and obducted to form ophiolites, and smaller fragments may get caught up in subducted sediments or serpentinites and come up to the surface as *mélange*.

Farther toward the volcanic front occurs a gently sloping area known as the *fore-arc*, which can be 100–200 km wide. Igneous activity has been noted in some fore-arcs, but this is rare. The isotherms in Fig. 3A illustrate how cool lithosphere is gently warmed as

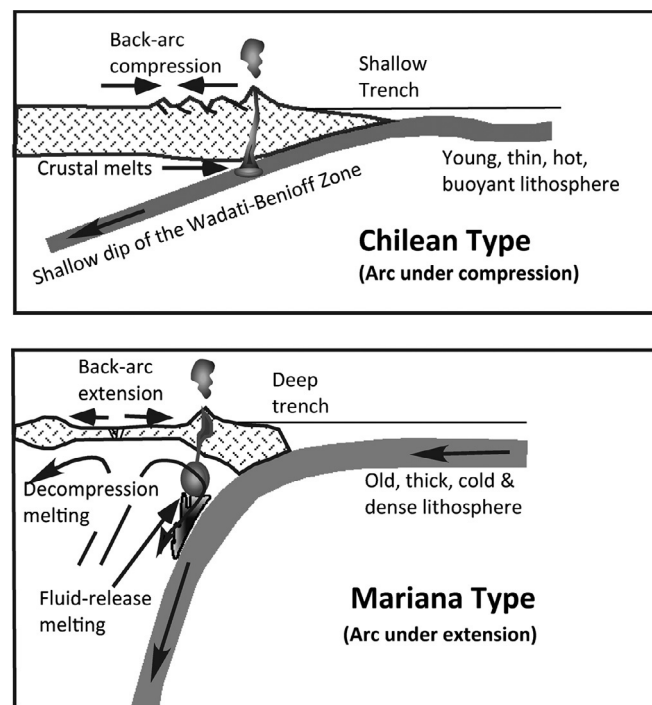


Fig. 2 Schematic cross-sections of two very different types of subduction zones—Chilean and Mariana type. From Stern RJ (2002) Subduction zones. *Reviews of Geophysics* 40. doi: 10.1029/2001RG000108.

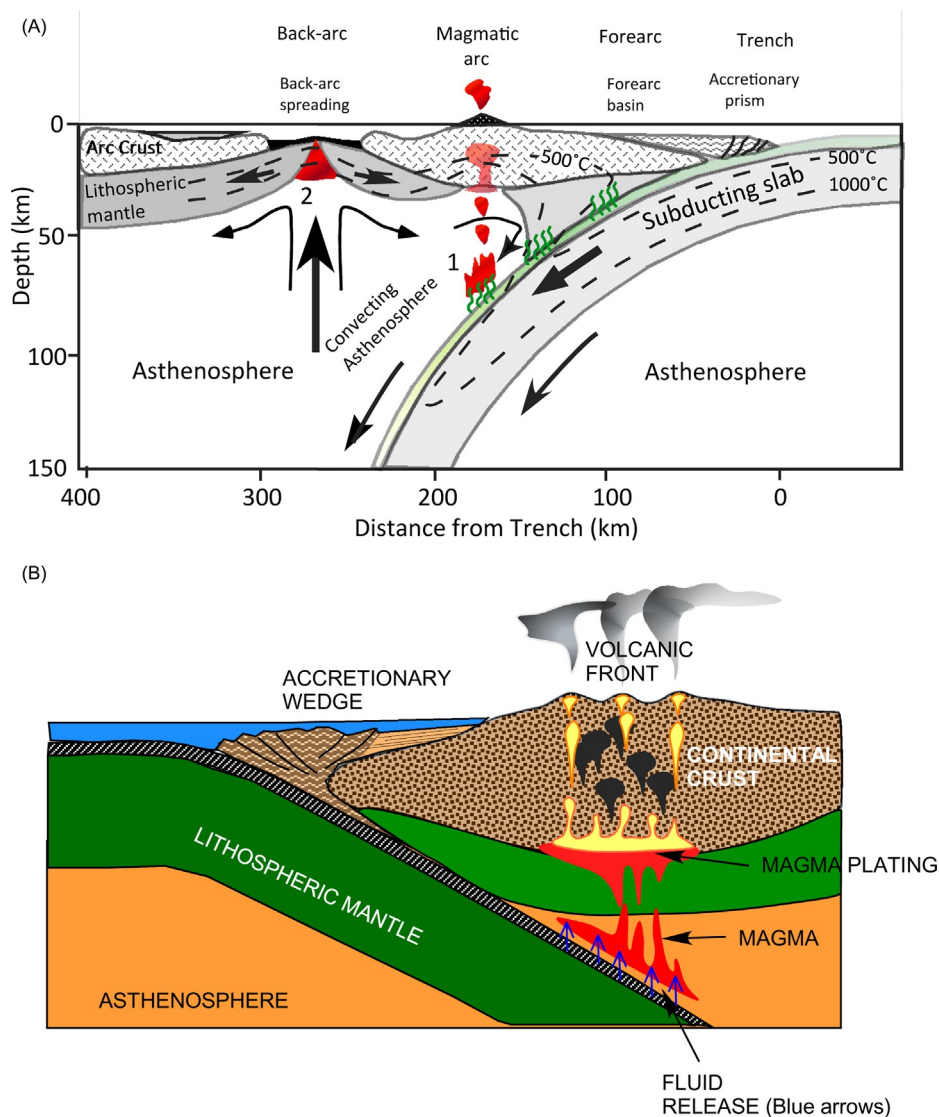


Fig. 3 (A) Schematic cross-section of an island arc highlighting its essential elements. The green squiggly lines represent fluids released from the subducting slab. Red = magmas. Two isotherms are also shown to illustrate how the thermal conditions change from beneath the arc to the subducting plate. (B) Schematic cross-section of a continental arc. It shows a thick and deformed accretionary prism in the fore-arc region between the trench and the arc. Hydrous fluids released from the subducting crust and melts derived from sediments rise into the mantle wedge and cause partial melting. These magmas underplate the Moho: here magma batches undergo mixing, assimilation of wall rocks, and partial crystallization. Evolved residual magma rises to form plutons (black) or erupts through volcanoes (yellow paths). From Stern RJ (2002) Subduction zones. *Reviews of Geophysics* 40. doi: 10.1029/2001RG000108.

it penetrates deeper into the mantle. In the basic scenario, ocean water enters through fractures in the crust and the shallow mantle close to the ridge axis where the ridge is still hot. The heated water reacts with the anhydrous minerals of the lithosphere and converts them into hydrous minerals like zeolites, chlorite, serpentine, which contain significant amounts of water (commonly ~13–14 wt% H₂O) in their respective atomic structures. More water is carried in sediments deposited on the oceanic plate, and water is also introduced into the subducted slab as a result of bending-related faulting just seaward of the trench.

As this partially hydrated plate is subducted into hot mantle known as asthenosphere, the increasing temperature and pressure destabilize the hydrous minerals, which break down and release water into the *asthenospheric wedge* or *mantle wedge* above the subducting plate. This added fluid lowers the melting temperature of the hot peridotite of the asthenospheric wedge and thus magma is formed (Fig. 3). This phenomenon is known as *fluid-fluxed melting*. Melting of sediments on the top of the subducted slab also contributes to this flux, which contains most of the incompatible trace elements that are carried up into convecting asthenosphere in the mantle wedge. A variation on this theme calls for the addition of slab-derived fluids and sediment melts that generate small amounts of hydrous melts closer to the slab, which then rise to stimulate production of much larger volumes of magma in the mantle wedge. The magma so formed rises due to buoyancy, and after undergoing some crystallization and contamination by the overlying crust, erupts through the volcanic front. Deeper plutons also form beneath the volcanic front

when magma batches solidify at depth. Granitoid plutons and rhyolitic volcanism in continental arcs generally form due to melting of the deep continental crust. Such melting occurs as the primary basaltic to andesitic magmas stall at the Moho and release heat to the overlying silicic crust, eventually leading to melting of the crust and formation of granite magma. To be sure, not all granites form this way and some silicic magmas form by crystal fractionation, assimilation and magma mixing.

Finally, although fluid-fluxed melting is the most important mechanism for generating magmas above subduction zones, decompression melting also occurs in some places, e.g., the back-arc area of the IBM arc (Figs. 2 and 3A). Here extension in the back-arc causes asthenosphere to rise (i.e., decompress) and melt to produce basalt magma, which creates new crust in the back-arc basin.

For an explanation of fluid-fluxed and decompression melting, see <https://www.youtube.com/watch?v=LqVWXRTcSiA>. The above themes are elaborated further in the following sections.

Magmatism in Arcs

Lavas

Many different types of lavas erupt from arc volcanoes—basalts, basaltic andesites, andesites, and rhyolites, with andesites being most diagnostic of arc volcanism. Their corresponding plutons are generally more intermediate to felsic in composition, and hence, we broadly group them as granitoid plutons.

The basalts associated with arc volcanism generally contain more Al_2O_3 than basalts erupted at mid-oceanic ridges or at hot spots like Hawaii, and are called *High-Alumina Basalts (HAB)*. Some strongly alkalic lavas also erupt, but they mostly occur farther away from the trench, in what is known as the “back arc.” Felsic magmas are common in arcs but these generally do not build volcanoes that rise above sea-level and their volumetric significance is often underappreciated. Rhyolites are more common in continental arcs. Granitoid and intermediate composition plutons form a major part of arcs, but these are only exposed on continents, where erosion has removed the volcanic carapace, as for example in the Sierra Nevadas of California.

The term “Igneous rock series” refers to the range of lava compositions, from basaltic to rhyolitic, from a single volcano or from a group of volcanoes situated in a particular geographic area. Initially, there was an underlying assumption that the mafic-intermediate-felsic lavas of a series are all related by some sort of fractional crystallization differentiation of a common parent magma (such as reflected in the minerals of Bowen’s reaction series); however, many studies of volcanic arcs have shown that is often not the case and that more complex processes, such as melting and assimilation of the crust associated with fractional crystallization are involved in the derivation of different magma types.

Several classification schemes have been proposed for arc igneous rocks among which two—based on FeO^*/MgO vs. SiO_2 and K_2O vs. SiO_2 —are commonly used (Fig. 4). The FeO^*/MgO vs. SiO_2 distinguishes between the tholeiitic series and calc-alkaline series (Fig. 4A). Lava compositions, commonly ranging from basaltic andesite to rhyolite, from several Chilean volcanoes are shown as trends in Fig. 4B—the *low-K series*, the *medium-K series*, the *high-K series*, and the *shoshonite series*. The low-K series is often referred to as the *island arc tholeiite series*, which is different from the tholeiitic basalts that erupt at mid-oceanic ridges and other extensional plate boundaries or at ocean islands (e.g., Hawaii). The main difference is that the island arc tholeiites show mild Fe-enrichment accompanied by SiO_2 -enrichment (i.e., Bowen trend), whereas “true” tholeiites (MORB, Hawaii, Deccan Traps types) show strong Fe-enrichment at a fairly constant SiO_2 (the Fenner trend). The high-K and shoshonite series, by virtue of their high alkali contents, are special types of alkaline series. Within each series, the rocks may range from basalt through andesite to rhyolite. Also shown in Fig. 4 are compositional trends of lavas erupted from several volcanoes from the Izu-Bonin-Mariana (IBM) arc. The Mariana lavas exhibit calc-alkaline trend, whereas Izu-Bonin lavas follow an island arc tholeiitic trend (Fig. 4B). The Andean lavas tend to start out in the calc-alkaline field but then become much richer in K_2O with increasing SiO_2 . Such enrichment may result from crustal contamination.

The eruption behavior of arc volcanoes is highly variable and is related to the igneous series: tholeiite series volcanoes are generally less explosive and erupt basalts and basaltic andesites from small, youthful cones and shield volcanoes. Because arc volcanoes erupt water-rich, high-silica magmas, the most violent eruptions happen at arc volcanoes (Stern et al., 2016). Tholeiitic rocks contain fewer large crystals—phenocrysts—than calc-alkaline series lavas. Calc-alkaline series volcanoes are generally explosive and commonly erupt pyroclastic materials. They often form large stratovolcanoes that dominate mature arcs, such as Fujiyama in Japan and Mt. Rainier in the Cascade Arc. The lavas commonly contain abundant phenocrysts of plagioclase. Late-stage volcanic activity in an arc is often of the very enriched shoshonite type. Shoshonite series volcanoes are minor relative to those of the tholeiitic and calc-alkaline series. Like calc-alkaline volcanoes, they are explosive as well.

Aside from the rock types mentioned above, a rather unusual type of lava, called *boninite*, with ~6–12% MgO and 52–60% SiO_2 occurs in some fore-arc regions of the IBM convergent margin. Boninite magmas are thought to form as a result of unusually high degrees of mantle melting, for example when a subduction zone first forms. They show strong enrichment in certain incompatible trace elements, such as large-ion lithophile elements (LILE) and are generally believed to form when H_2O and LILE are added to previously depleted asthenospheric wedge. In 2009, boninite lavas were observed for the first time to erupt from the West Mata volcano, which is the deepest known volcano known (1.1 km below sea level) and is located behind the Tonga arc in the Lau backarc basin. A video of Mata volcano erupting underwater can be seen at <https://www.youtube.com/watch?v=xRaEcGHHsVY>

There is another special type of arc lava called *Adakite*, named after Adak Island in the Aleutian Islands of Alaska. Adakites are found where the subducting plate is very young and still warm. They are compositionally andesites, with >56% SiO_2 , >15% Al_2O_3 ,

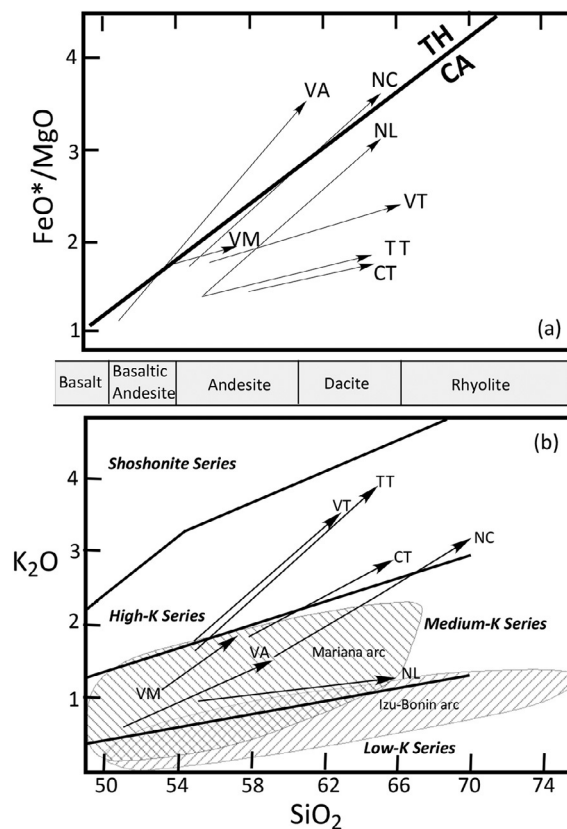


Fig. 4 Classification of volcanic rocks from convergent plate boundaries on the basis of weight percent concentrations of major oxides: (A) FeO^*/MgO vs. SiO_2 , and (B) K_2O vs. SiO_2 . In (A) only two types are recognized—calc-alkaline (CA) and tholeiitic (TH). (B) the fields for four major igneous series—Low-K, Medium-K, High-K, and Shoshonite series. The middle bar between (A) and (B) shows the corresponding names of volcanic rocks. Compositional trends in lavas erupted from several volcanoes in Chile are also plotted here: CT: Cerro Tupungoto; TT: Volcan Tupungatito; VM: Volcan Maipo; VT: Volcan Tinguiririca; SL: Cerro Sordo Lucas; AZ: Cerro Azul; NL: Nevado de Longavi; NC: Nevados de Chillan; VA: Volcan Antuco. Hildreth W, and Moorbath S (1988) Crustal contributions to arc magmatism in the Andes of Central Chile. *Contributions to Mineralogy and Petrology* 98: 455–489.

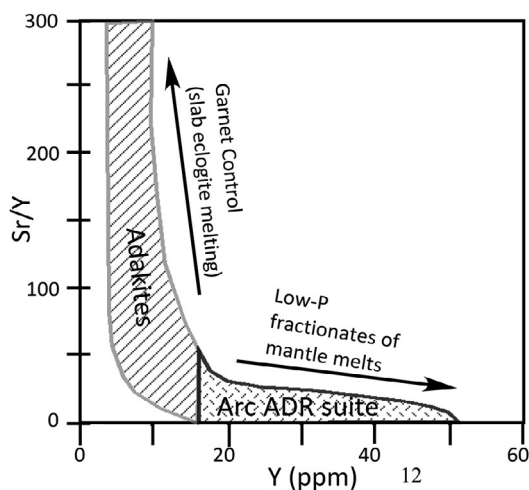


Fig. 5 Trace element diagram showing the distinctive chemical characteristics of adakites, namely, strong variation in Sr/Y ratio over a very small range of Yb (ppm). Stern RJ (2002) Subduction zones. *Reviews of Geophysics* 40. doi: 10.1029/2001RG000108.

and about 3% MgO; but what makes them distinctive is their unusually high Sr/Y and La/Yb ratio (Fig. 5). The high Sr/Y and La/Yb ratios are interpreted to be a result of melting of eclogitic crust in the subducted slab. Y and Yb are concentrated in garnet, whereas Sr and La are incompatible elements and concentrate in the melt. Therefore, during melting of the subducting eclogite crust, residual garnet sequesters Y and Yb and increase La and Sr in the melt, which results in high Sr/Y and La/Yb ratios in adakite melt.

Phenocryst Mineralogy

The mineralogy of island arc lavas varies as a function of silica content and series type: olivine (Fo₇₀₋₈₅), augite and a Ca-rich plagioclase (>90% anorthite) are common phenocrysts in basalt and basaltic andesites. Brown hornblende and biotite are common phenocrysts in andesites, dacites and rhyolites of calc-alkaline and high-K series. These hydrous mineral assemblages suggest relatively high H₂O contents of the magmas. In contrast, low-K-series andesites contain phenocrysts of orthopyroxene or pigeonite. Crystallization of pigeonite requires temperatures that are substantially higher than the temperatures at which hydrous mafic-intermediate magmas may crystallize at a moderate-to-low pressure. Therefore, the occurrence of orthopyroxene and pigeonite in the low-K series suggests that the low-K series (i.e., island arc tholeiitic series) magmas have less H₂O compared to the other series. Plagioclase, which is a dominant phenocryst in calc-alkaline and low-K basalt and andesite, is not nearly as common in high-K and shoshonite series lavas. Pigeonite is a common groundmass mineral in the low-K or tholeiitic series, whereas orthopyroxene is the common groundmass Ca-poor pyroxene in andesites. Sanidine (\pm fayalitic olivine) may also occur as a phenocrysts in rhyolites.

Trace Element Composition

Trace element characteristics are commonly displayed in terms of the so-called “spider diagrams” or “spidergrams” in which elemental concentrations, normalized to primitive upper mantle or MORB compositions, are plotted (Fig. 6A and B). Arc basalts including tholeiites, back-arc basin basalts, and even boninites, are distinct from N-MORB and hot spot or ocean island basalts (e.g., Hawaii) by their conspicuous spiky patterns, characteristic enrichments in some strongly incompatible elements (e.g., cesium and barium), and depletion in niobium (Nb) content relative to the adjacent elements. Elements such as Cs and Ba are fluid-mobile elements, which dissolve into fluids or fluid-saturated melts released from the subducted crust and are transported up into the

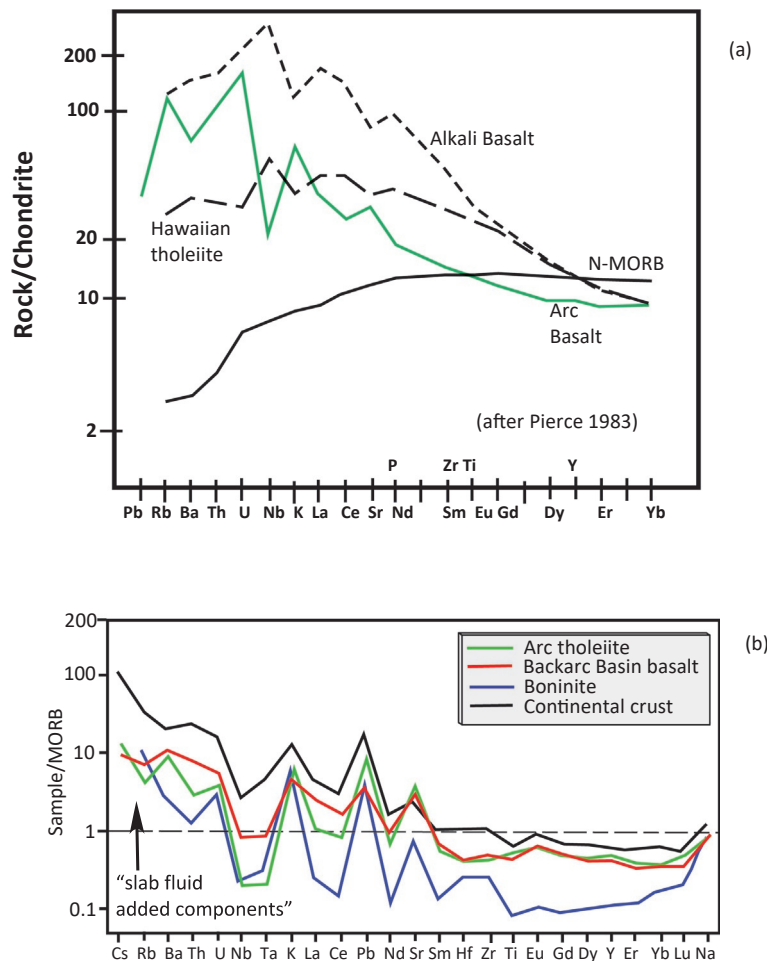


Fig. 6 “Spider diagrams” showing trace element compositions of (A) basalts from various hot spots (e.g., alkali basalt and Hawaiian tholeiite), normal mid-oceanic ridges (N-MORB), and island arc (arc basalt); and (B) of arc volcanics. Note that the rock compositions are normalized to the composition of a chondritic meteorite in (A) and to N-MORB in (B). Estimated compositional range of fluids coming off subducted slab is also shown in (B). After (A) Pearce J (1983) Role of the sub-continental lithosphere in magma genesis at active continental margins. In: Hawkesworth CJ and Norry MJ, eds. *Continental Basalts and Mantle Xenoliths*, Nantwich, Cheshire: Shiva Publications, pp. 230–249; (B) Stern RJ (2002) Subduction zones. *Reviews of Geophysics* 40. doi: 10.1029/2001RG000108.

hotter parts in the asthenospheric wedge where these elements are added to magma. This process is primarily responsible for the jagged pattern and LILE enrichment in arc magmas (Fig. 6B).

Arc lavas generally show a flat middle rare earth element (MREE) and heavy rare earth element (HREE) (chondrite-normalized) pattern, which indicates that garnet is not a residual phase in the magma generation process. An exception to this is adakite magma, which has a high MREE/HREE ratio and hence is likely to have been generated with residual garnet.

The strong depletion in REE in boninites suggests they are derived from a strongly depleted peridotite source relative to that of mid-ocean ridge basalt (MORB). The combination of high fluid-mobile element concentrations and depleted REE indicates that boninite magmas are generated from a harzburgite (depleted mantle) source to which fluids from the subducted slab have been added.

Isotope Composition

In terms of Pb-, Nd- and Sr-isotopic compositions, igneous rocks from several island and continental arcs define a rather wide field that overlaps the fields of N-MORB, hot spot basalt, oceanic sediments and continental crust (Fig. 7A and B). Such great isotopic diversity signifies two things: (a) materials for arc magmas are contributed from a variety of sources—asthenosphere (i.e., N-MORB source), mantle plumes (OIB source), oceanic sediments, and continental crust (in the case of continental arc volcanics); and (b) different arcs can have very different isotopic compositions indicating that the relative material contributions from these different sources can vary from arc to arc. The physical means by which such “contributions” are made, for example, whether during melting in the subduction zone or through contamination of transient melts by the crust, is not often easy to discern.

Large Ignimbrite Eruptions: The Long Valley Caldera Example

An important feature of continental arc volcanism is giant eruptions of rhyolite that can cover thousands of km²: for example, the Bishop Tuff eruption (Fig. 8A) from the Long Valley Caldera (LVC) located at the boundary between the Sierra Nevada and the Basin and Range Province (Fig. 8B). Although this is not associated with an active subduction zone, the LVC is a useful example of giant rhyolite arc eruptions. About 760,000 years ago the volcano blew out its roof, formed the caldera, and poured out rhyolitic lava, pyroclastic flows, and ash. The ash spread as far as Nebraska (Fig. 8A). The thick welded pyroclastic deposit that formed due to this cataclysmic event is known as the Bishop Tuff.

Large ignimbrite eruptions are triggered by vapor saturation of magma in large silica-rich magma chambers. Shallow crustal silicic magma chambers cool and crystallize along the walls, creating a mush of crystals and melt, with the proportion of melt and

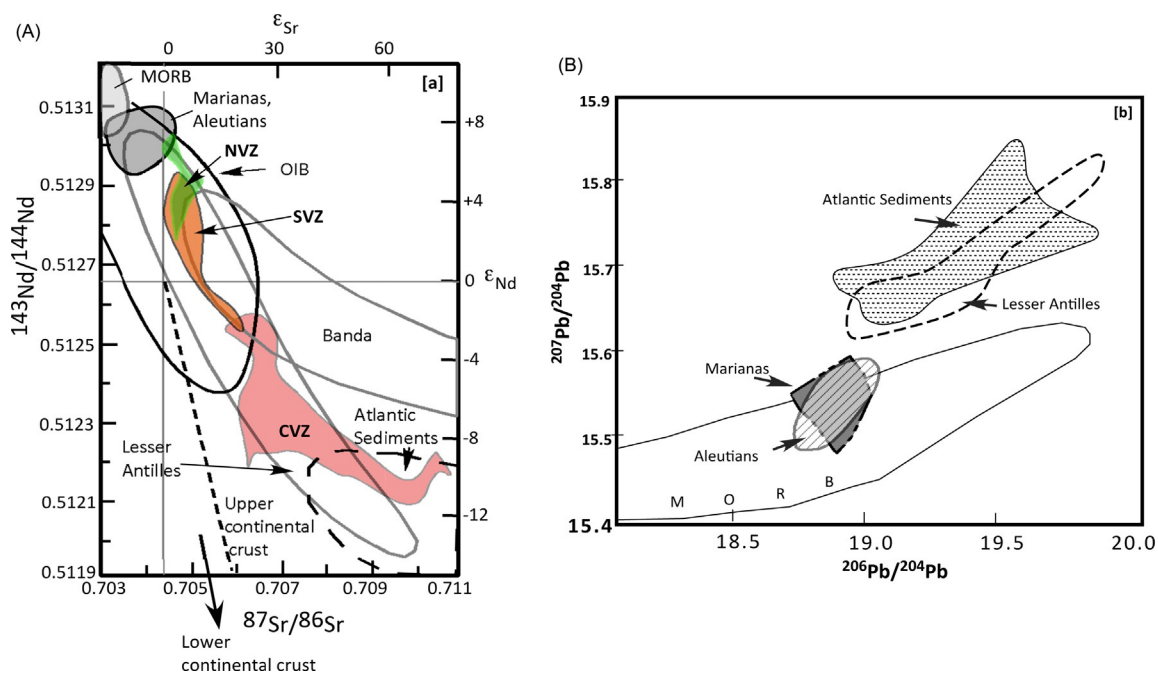


Fig. 7 (A) Nd-Sr isotopic compositions of arc volcanics from different convergent margins are compared with those of MORB, continental crust, Atlantic ocean bottom sediments, and ocean island basalts (OIB). Arc lavas from three volcanic zones from the Andes are shown as NVZ (Northern Volcanic Zone), SVZ (Southern Volcanic Zone), and CVZ (Central Volcanic Zone). Whereas Marianas and Aleutian volcanics appear to have not been affected by continental crust-derived sediments, those from the CVZ, Lesser Antilles, and Banda arc (Indonesia) appear to have a strong continental crustal signature. (B) Pb-isotope compositions of selected arc volcanics. After Wilson BM (2007) *Igneous Petrogenesis: A Global Tectonic Approach*. Netherlands: Springer Netherlands, 466 p.

Large Ignimbrite Eruptions: The Long Valley Caldera Example

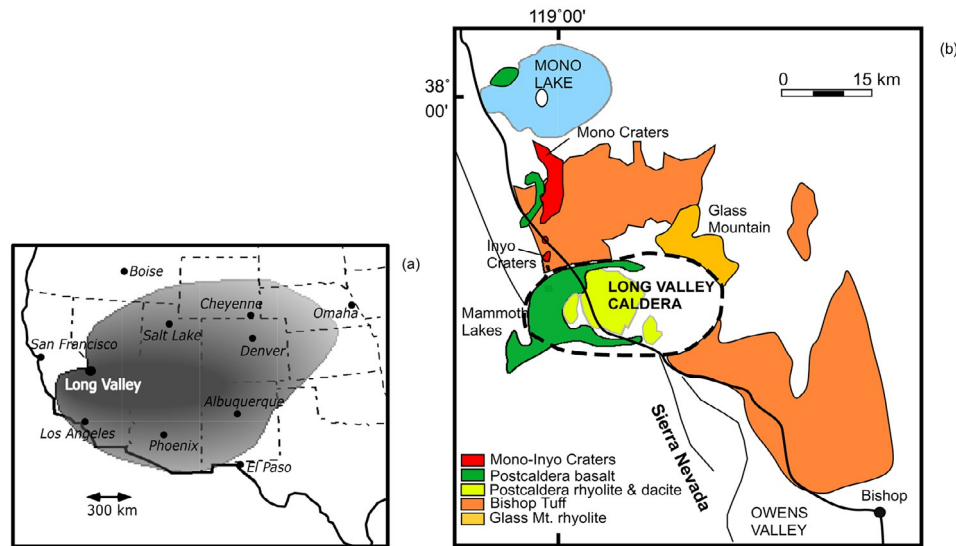


Fig. 8 (A) Spread of ash (in gray) of the Bishop Tuff eruptive event from the Long Valley Caldera. (B) Simplified map of the Long Valley Caldera system.

vapor increasing toward a melt-rich “lens” near the roof of the chamber. Compaction contributes more melt to the lens by squeezing out the interstitial melt from the mush zone. Such processes can operate over hundreds or thousands of year timescales. The result is a giant vapor-saturated melt lens near the roof of the magma chamber. Exsolution of vapor bubbles from the cooling melt leads to accumulation of a vapor-rich melt layer near the roof. Eventual collapse of the roof leads to explosive eruption of an ignimbrite, which is a mixture of ash, glass shards, and solid particles (crystals in the chamber and overlying roof materials). The bulk of the material erupted this way comes from the shallowest part of the magma chamber; and with time deeper materials (lava and pyroclastics) are erupted.

The LVC is part of a larger volcanic system whose activities started about 4 million years ago and continues today (Fig. 9; Bailey, 2004). Much of what is described here comes from Bailey’s summary of this volcanic system. Fig. 9 shows the timing, volume, and type of eruptions that occurred over the last 4 million years over an area within 10 km of the LVC.

The early precaldern volcanism led to laterally extensive basalt-trachyandesite lava flows. On the rim and within the caldera the igneous activity began forming dacite domes, flows, and tuffs. The volcanism became rhyolitic and produced the Glass Mountain on the northern rim of the LVC.

After the roof collapsed, the magma chamber received new magma and inflated, forming the resurgent dome within the caldera. Rhyolite continued to erupt as lava flows, domes, and tuffs on the floor of the caldera. Basalt enclaves were found in the rhyolite. Basalt-dacite lava flows erupted from the rim of the caldera and from the neighboring Inyo-Mono craters associated with a fissure system (Fig. 8B).

Composition of Precaldern, Bishop Tuff, and Postcaldera Lavas

Bailey (2004) noted significant differences between the Precaldern lavas that erupted from Central Sierra, East Sierra, and the Basin & Range area (Fig. 10). The basalts from the three areas are alkalic in character and are high in K_2O ; and they form subparallel trends in the TAS diagram, indicating the presence of at least two different parent magmas in each case. The East Sierra suite of lavas exhibits distinct compositional gaps between basalts, trachyandesites, and dacites. The postcaldera lavas, from basalts to rhyolites/alkali rhyolites, overlap the precaldern lava suites from the Basin & Range and eastern Sierras. The precaldern basalts are distinctly more magnesian than the postcaldera basalts, although the more evolved pre- and postcaldera lavas overlap in composition (Fig. 10B). In terms of REE, precaldern basalts show steeper LREE enrichment and lower HREEs (Fig. 10C).

Detailed studies of the Bishop Tuff have been carried out by many different groups (references in Hildreth and Wilson, 2007). It has been determined that the Bishop Tuff eruption event lasted only 6 days. The Bishop Tuff has the composition of a high-silica rhyolite ($SiO_2 = 74\text{--}78\%$) and is composed of ash and pumice clasts containing biotite, plagioclase, sanidine, and quartz (Hildreth and Wilson, 2007). Early studies of layers within the Bishop Tuff by Hildreth and co-workers suggested that the LVC magma chamber was zoned in terms of its chemistry, temperature, and crystal content, and such zoning is recorded in the vertical layering of the Tuff. A vast body of literature exists debating the processes that might have contributed to the formation of such a zoned rhyolitic magma chamber. More recent studies have found, however, that such a simplistic picture needs rethinking. Hildreth and Wilson (2007) found that the proportion of crystals increased and so did the temperature ($714\text{--}818\text{ }^\circ\text{C}$) with time. They suggested

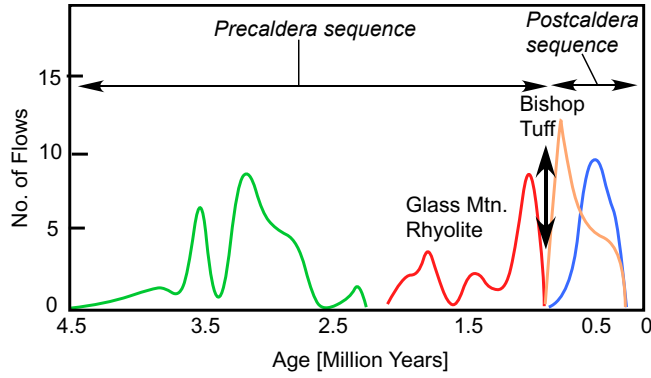


Fig. 9 Age and frequency of flows from the LVC system. Bailey RA (2004) Eruptive history and chemical evolution of the precaldera and postcaldera basaltic-dacite sequences, Long Valley, California: implications for magma sources, current magmatic unrest, and future volcanism, U.S. Geological Survey Professional Paper 1692, 76 p.

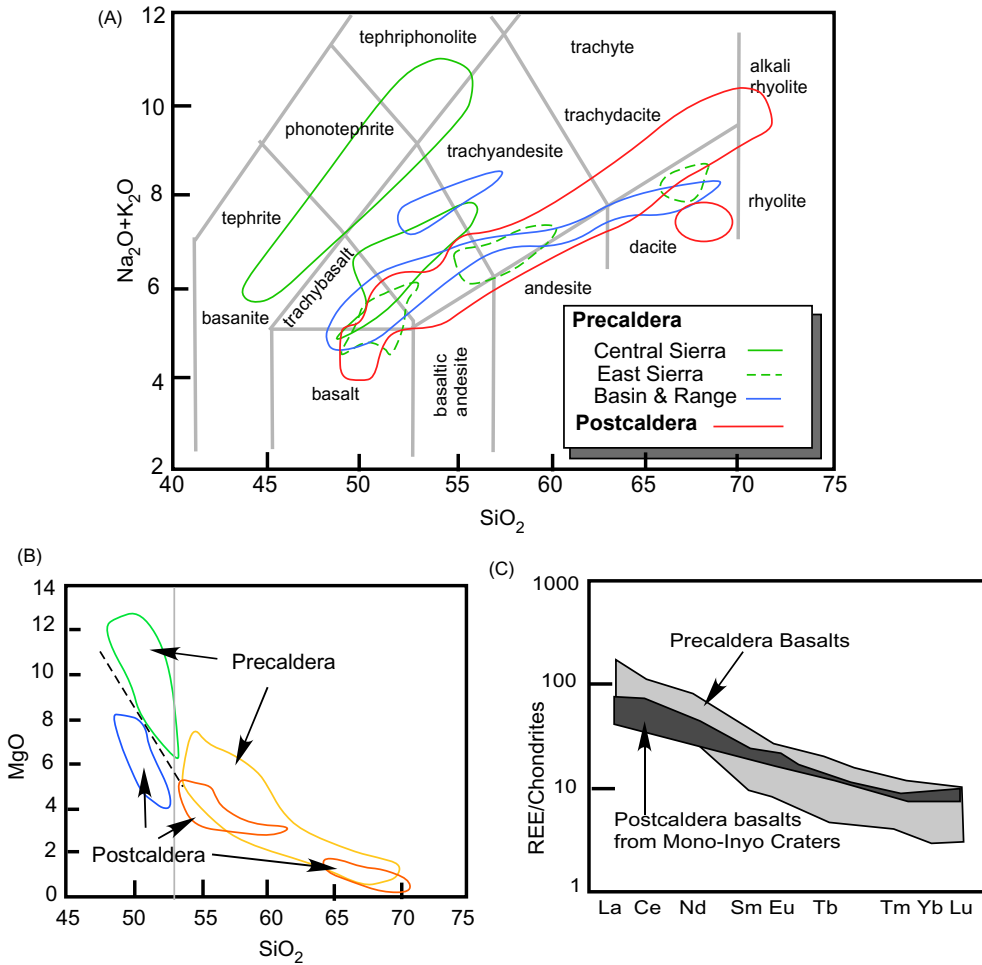


Fig. 10 (A) Composition of lavas erupted from the Long Valley Caldera on the total alkalis-silica (TAS) diagram (B) MgO-SiO₂ variation shown by Precaldera and Postcaldera lavas erupted from the Long Valley Caldera. (C) Comparison of REE patterns of Precaldera and Postcaldera basalts. Bailey RA (2004) Eruptive history and chemical evolution of the precaldera and postcaldera basaltic-dacite sequences, Long Valley, California: implications for magma sources, current magmatic unrest, and future volcanism, U.S. Geological Survey Professional Paper 1692, 76 p.

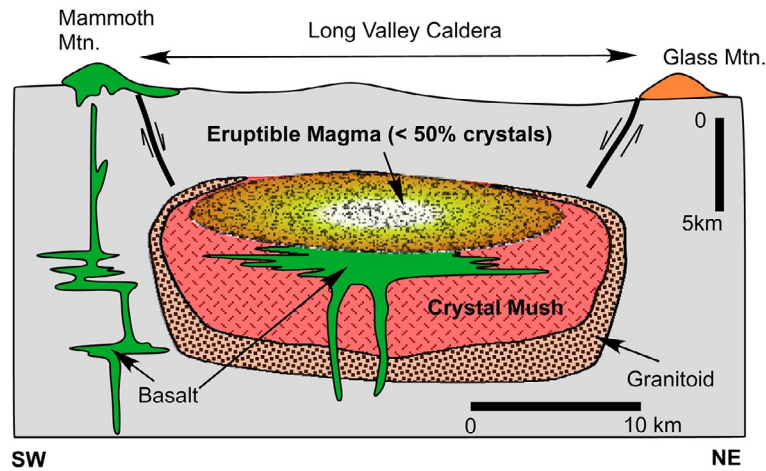


Fig. 11 Schematic cross-section showing the physical nature of the magma chamber beneath the Long Valley Caldera. Redrawn from Bachmann O, and Bergantz GW (2004) On the origin of crystal-poor rhyolites: Extracted from batholithic crystal mushes. *Journal of Petrology* 45: 1565–1582.

that shortly before the Bishop Tuff eruption, the crystal-rich melt lens at the roof of the LVC was intruded by fresh, hotter, crystal-poor batches of low-silica rhyolite.

A simplified model magma chamber for the LVC is shown in Fig. 11 (source: Bachmann and Bergantz, 2004), which summarizes the observations presented above. Crystallization led to the formation of a melt lens with less than 50% crystals near the roof of the chamber. This is the only “eruptible” part of the chamber. The rest of the magma chamber has less than 50% melt, which means that the crystals are interlocked with melt occurring between the crystals. What triggered the Bishop Tuff eruption is possibly the overpressure created by exsolved gases from the melt, augmented by new supply of heat and gases brought in by fresh batches of hotter magma (basaltic, dacitic, as well as rhyolitic).

Plutons

Granitoid batholiths are elongated belts that cover areas of approximately thousands of km² and form the plutonic core of continental arcs. These batholiths are composed of many individual plutons and are only exposed when deep erosion removes the volcanic carapace and exposes the roots of the arc. It is a common practice to use the broad term “granitic” or “granitoid” (instead of granite) to refer to plutonic, coarse-grained igneous rocks that are composed dominantly of various proportions of quartz, alkali feldspar, and plagioclase feldspar, with minor amounts of other minerals such as hornblende or biotite. In reality, however, based on classification by the International Union of Geological Sciences, the formal rock names may vary from tonalite, quartz diorite, granodiorite, to quartz monzonite, and granite. The exposed surface area of a granitoid pluton is related to the shape, volume, and extent of erosion. The plan view of granitoid plutons can vary from circular to elliptical to dike-like (cf. Clarke, 1992). Their three-dimensional structure is generally difficult to determine; however, geophysical studies and analogue model experiments indicate that they vary from dome, tabular, mushroom, to inverted teardrop shapes (Clarke, 1992; Pitcher, 1993). The Sierra Nevada batholith of the United States (Fig. 12) and the coastal batholiths of Peru and Chile are excellent examples of continental arc batholiths.

An arc batholith is not a homogeneous body but is composed of many smaller (commonly 2–50 km²) plutons that are emplaced over millions of years. The magma composition with each phase of intrusion changes as well. The coastal batholith of Peru consists of a chain of 800 plutons that were emplaced over a period between 110 and 30 million years ago.

The Tuolumne Intrusive Series, a relatively small pluton found in Yosemite Valley within the Sierra Nevada batholith, witnessed at least four distinct episodes of magma emplacement (Bateman and Chappell, 1979). A hornblende + biotite bearing quartz diorite occurs at the peripheral region and was the first batch of magma to be emplaced. The intermediate region is composed of granodiorite, and porphyritic granite occurs at the core of the pluton. Bateman and Chappell (1979) showed that these distinct episodes of magma intrusion occurred in the core region of the pluton while the pluton was still not fully solid. Intrusion of younger magma batches resulted in episodic breaching of the solid margins of the intrusion.

Sierra Nevada Batholith (SNB)

The Sierra Nevada Batholith dominates the eastern flank of California and the western edge of Nevada (Fig. 12). It is generally accepted that the western half of the SNB resides on juvenile oceanic crust whereas the eastern SNB intrudes the North American craton. The ⁸⁷Sr/⁸⁶Sr = 0.706 line in the batholith divides the two crust types.

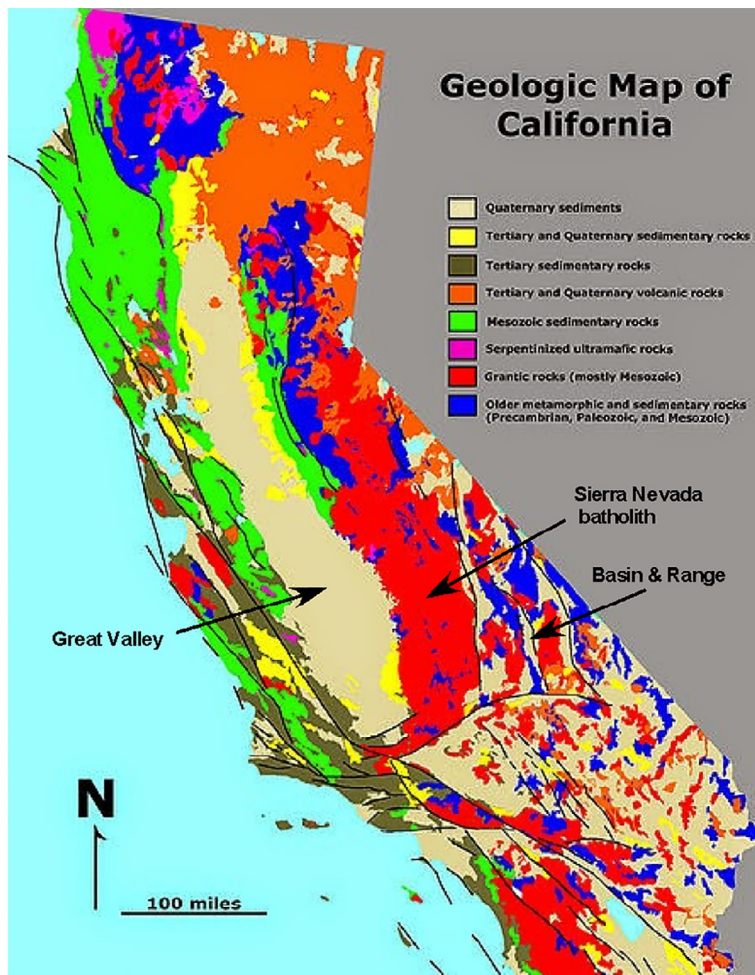


Fig. 12 Map of the Sierra Nevada Batholith.

The SNB formed as a result of igneous activity related to the subduction of the Farallon Plate beneath the North American Plate some 220–80 Ma. Two short-lived magmatic episodes - one at 160–150 Ma and the other at 100–85 Ma built most of the batholith. Plutons comprising the SNB are composed of tonalites, granodiorite, and granite. Gabbro, diorite, and leucogranite plutons are small and probably comprise no more than 2% of the outcrop (Lee et al., 2006, and refs. therein). Geobarometry indicates that this granitoid batholith was originally about 35 km thick. The top 5–6 km of its volcanic cover and some of the batholith have been removed by erosion.

There is a significant body of information on the deeper parts of the batholith from sections exposed in the southern SNB, seismology, and from xenoliths brought up by recent volcanism. These xenoliths include garnet pyroxenites, garnet peridotites, spinel peridotites, plagioclase peridotites, garnet granulites, and some metasedimentary rocks thought to represent the roots of the SNB. Garnet pyroxenites are the most abundant type of xenolith and are of two types (Fig. 13)—high-MgO pyroxenites and low-MgO pyroxenites. High-MgO xenoliths are cumulates from hydrous basaltic magmas (Lee et al., 2006), and low-MgO xenoliths were postulated to be residues of crustal melting that generated the felsic melts of the SNB (Ducea, 2001; Saleeby et al., 2003).

Primary Magmas and Daly Gap

How arc magmatism works requires an understanding of the nature and conditions of origin of primary magmas in a subduction setting, and how such magmas relate to erupted lavas. In this regard, the Cascades volcanic arc of western United States and Canada presents a fascinating case where primitive near-aphyric (molten or nearly molten when erupted) lavas with $Mg\#$ ($= 100 \text{ Mg}/(\text{Mg} + \text{Fe}^{2+})$ in atomic proportions) as high as 70–75 occur (Leeman et al., 2005; Fig. 14). They also have high Ni and Cr contents. Mg/Fe partitioning suggests that such lavas could be “primary,” meaning these magmas were in equilibrium with mantle peridotite, which could be the asthenosphere or the mantle section of the overriding plate. Leeman et al. (2005) identified two major chemical groups—Group II has greater $Mg\#$ than Group I (Fig. 14), as high as 75 for Group II and 68 for Group I. Group I has chemical

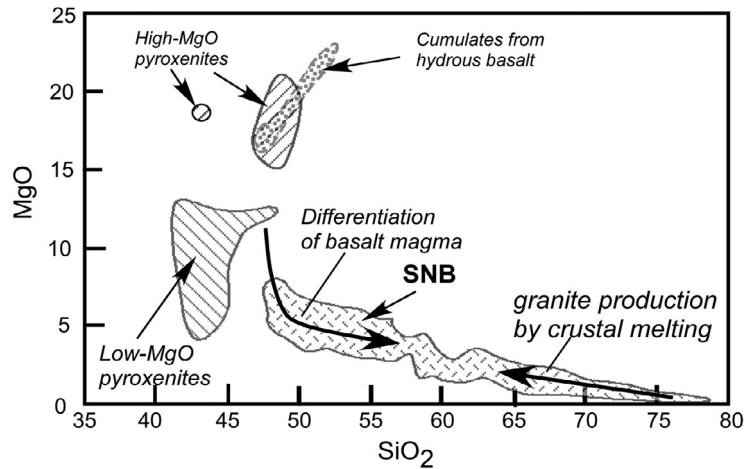


Fig. 13 Compositions of the two types of garnet pyroxenite xenoliths and the Sierra Nevada Batholith (SNB). Composition of cumulates in experimental crystallization of hydrous basalts is also shown. The arrows suggest that the low-silica granitoids in the SNB may have largely formed by fractional crystallization of basalt magma; and the high-silica granitoids have formed by melting of the crust. After Lee C-TA, Cheng X, and Horodyskyj U (2006) The development and refinement of continental arcs by primary basaltic magmatism, garnet pyroxenite accumulation, basaltic recharge and delamination: Insights from the Sierra Nevada, California. *Contributions to Mineralogy and Petrology* 151: 222–242.

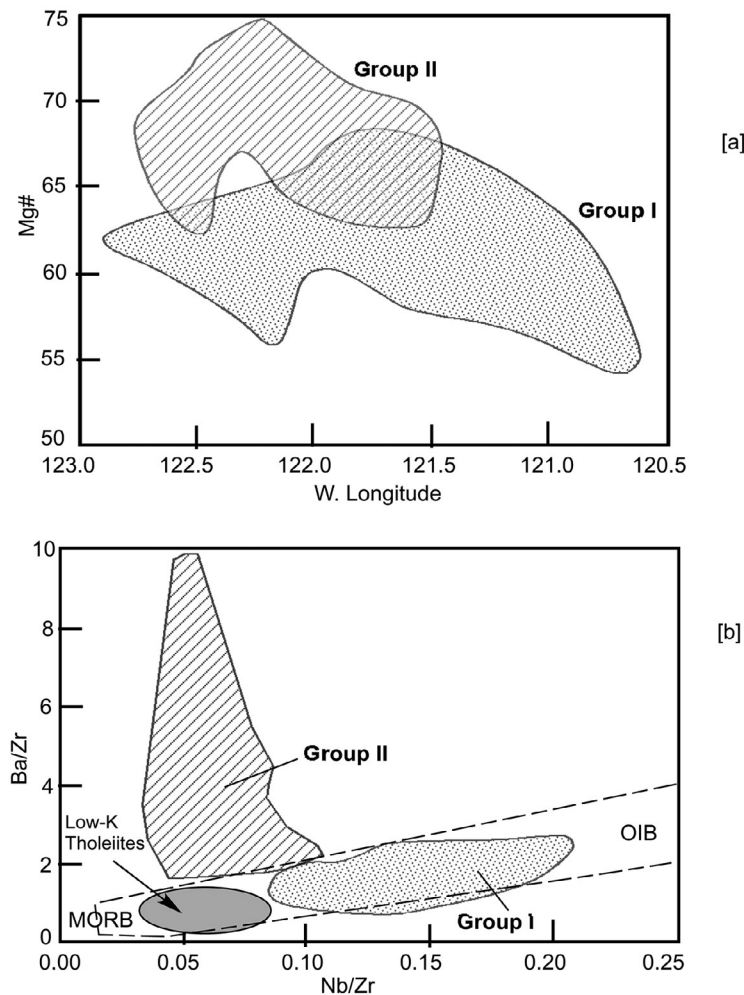


Fig. 14 Compositional groups of primitive Cascades lavas. (A) Mg# variations as a function of latitude, and (B) Ba/Zr vs. Nb/Zr variation. From Leeman WP, Lewis JF, Everts RC, Conrey RM, and Streck MJ (2005) Petrologic constraints on the thermal structure of the cascades arc. *Journal of Volcanology and Geothermal Research* 140: 67–105.

characteristics that are similar to MORB and/or OIB. Group II is enriched in Ba and depleted in Nb and thus resembles normal calc-alkaline arc lavas. Leeman et al. (2005) reconstructed primary magma compositions after correcting the lava compositions for possible fractionation so that they would be in equilibrium with mantle olivine. They also calculated the depth and temperature of equilibration of such primary magmas as follows: Group I—50–70 km, 1180–1280 °C, Group II—30–50 km, 1160–1300 °C. Leeman et al. (2005) noted that the bulk of both groups fall in the temperature range 1200–1250 °C. From this they drew two important conclusions: (1) Group I formed by decompression melting of the asthenosphere (and not by fluid-fluxed melting as is normally expected beneath volcanic arcs), whereas Group II formed by fluid-fluxed melting. (2) Group I formed deeper in the mantle wedge and may have been the heat source for generating Group II magmas, which of course required fluid from the descending slab as well. Leeman et al.'s first conclusion is particularly significant for warm subduction zones like the Cascades, where advection may be an important process in generating magmas in the asthenospheric wedge (cf. Kelemen et al., 2003). The decompression melting can happen in two different ways—by oblique upwelling accompanying return flow in the wedge due to the viscous coupling with the descending slab, or by diapiric rise of mantle+melt mixtures (review by Kelemen et al., 2003).

The Cascades arc may be an arc “end-member” because it formed due to slow subduction (4 cm/year) of the young (12–14 Ma) and warm Juan de Fuca and Gorda plates beneath the North American plate. The crust of the hot, downgoing slab is largely dehydrated and furnishes little fluid to the overriding plate. Also, whereas primitive lavas of the Cascades are virtually aphyric and highly magnesian ($\text{MgO} > 9\%$), arc lavas from other arcs are generally quite porphyritic and have lower MgO (2–5%). In this context, Leeman et al.'s (2005) conclusion has important implications for the nature of primary arc magmas and their generation.

If magmas from the asthenospheric wedge interact significantly with the sub-continental lithosphere and crust while going through crustal magma chamber processes, then erupted lavas must differ from the primary magmas from which they were derived. There are exceptions to this statement: for example, many rear-arc volcanoes exist away from the volcanic front and trench. These rear-arc volcanoes erupt alkali basaltic lavas (e.g., Japanese volcanic arc) carrying deep crustal and mantle xenoliths to the surface; this requires rapid magma rise so that these lavas are close to being primary. Nevertheless, xenolith-bearing alkaline lavas comprise a minor fraction of arc lavas.

Another unusual convergent margin magmatype is boninite. Primitive boninites (with 54% SiO_2 , $\text{MgO} > 10\%$) or their primary magmas form by hydrous melting of depleted lithosphere during early arc development (as discussed before), and although boninites occur in some ophiolites, it is likely that boninite magmas are volumetrically minor relative to andesites and basalts. The bulk of arc lavas form the calc-alkaline or medium-K series, and generation of their parent magmas is of greatest interest here.

An important approach toward deciphering the nature of primary magmas from arc volcanoes comes from studies of melt inclusions in phenocrysts. These inclusions are typically smaller than 100 μm in diameter and so must be studied with micro-analytical tools. The findings of a melt inclusion study by Reubi and Blundy (2009) is particularly relevant.

Reubi and Blundy (2009) constructed a SiO_2 -frequency plot of a large number of melt inclusions in different phenocryst phases and of whole rock samples from volcanic arcs worldwide using the GEOROC database (Fig. 15). The result was a clear bimodal distribution with two peaks corresponding to basalts and rhyolites; andesitic compositions are much less common. Whole-rock analyses of volcanic rocks do not exhibit such bimodal distribution and instead, we see a basaltic peak with a broader, smaller peak of andesitic composition. Reubi and Blundy (2009) hypothesized that the primary magmas produced at arcs are basalts and rhyolites, and that andesites are produced by mixing the two magma types. Other evidence presented in support of this hypothesis includes the following: (1) thermodynamically modeled or experimentally derived liquid lines of descent from primary basaltic magma do not go through andesite compositions, (2) linear trends exhibited by arc lavas on oxide-oxide or elemental plots are better explained by magma mixing, and (3) the common presence of disequilibrium phenocrysts and magma mingling/mixing texture in intermediate composition lavas. The melt inclusions contain a maximum of 6 wt% dissolved H_2O , regardless of whether the vapor-saturated inclusion was basaltic or rhyolitic. Their calculated minimum (minimum because they probably lost some vapor due to exsolution during ascent) entrapment pressure for such inclusions was about 0.5 GPa (18 km), indicating that the diverse melt inclusion compositions were acquired from greater depth—perhaps in the middle crust.

The gap or low frequency in andesitic composition is also known as the *Daly Gap*, after Reginald Daly who in 1925 noticed the dearth of igneous rocks between about 57% and 70% SiO_2 . The Daly Gap is not unique to arcs but also occurs in volcanic rocks associated with ocean islands (hot spots) and continental extensional zones. So, how does one explain the Daly gap in natural rock compositions, particularly with reference to volcanic arcs? Many proposals have been put forth, and some have been recycled over time as better-quality geochemical data from volcanoes and experimental studies have become available. We discuss a few here.

Grove and Donnelly-Nolan (1986) provided an interesting explanation, which followed an earlier suggestion by Peter Wyllie for the Daly gap at the Medicine Lake volcano (Cascades). They attributed the gap to the thermodynamics of fractional crystallization of basalt magma. Experimental crystallization of hydrated basalt magma at mid-lower crustal depth showed that the liquidus surface (i.e., $\Delta T/\Delta X$) flattens out sharply in T-X space as the liquidus surface $\text{Liq} + \text{Ol} + \text{Pl} + \text{Aug}$ gives way to $\text{Liq} + \text{Pl} + \text{Hbl} + \text{Opx} + \text{Oxide}$ (magnetite, ilmenite), and the slope steepens again when the melt composition becomes rhyolitic (Fig. 16). What this means is that andesitic melts can only form over a limited temperature interval during which large amounts of crystals (in this case, hornblende-orthopyroxene-plagioclase cumulate) must fractionate from parent basalt magma. Thus, one would see fewer andesites erupting from a fractionating basaltic magma chamber. Rhyolite volume should also be small as the residual liquid percentage at that stage will also be small.

A more commonly accepted explanation for the Daly gap is the production of granitoid magma by melting of the continental crust due to basalt magma pooled and stagnated (basaltic “underplate”) in the lower crust (Fig. 17). The heat is supplied from the ponded basalt magma in two ways—from the loss of its ambient heat (inherited from the mantle) and latent heat released by

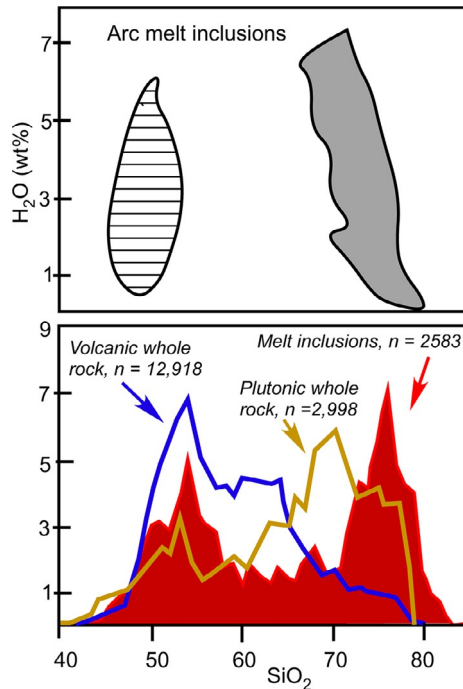


Fig. 15 Compositions of melt inclusions in phenocrysts in arc volcanics worldwide. Top diagram shows two distinct groups of melt inclusions with very different SiO₂ contents. Bottom diagram compares whole rocks with melt inclusions. Modified from Reubi O, and Blundy J (2009) A dearth of intermediate melts at subduction zone volcanoes and the petrogenesis of arc andesites. *Nature* 461: 1269–1273.

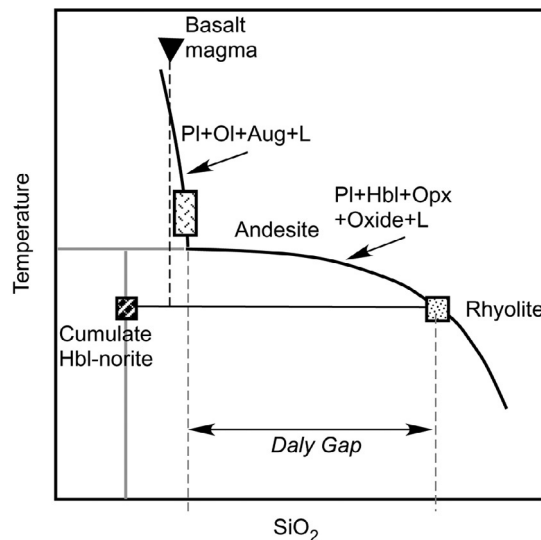


Fig. 16 Liquidus surface of a hydrous basalt. Redrawn from Grove TL, and Donnelly-Nolan J (1986) The evolution of young silicic lavas at Medicine Lake Volcano, California: Implications for the origin of compositional gaps in calc-alkaline lava series. *Contributions to Mineralogy and Petrology* 92: 281–302.

crystallization of mineral phases. This model works particularly well for continental extensional regimes where bimodal volcanism is a characteristic feature. Mixing between the fractionating basalt magma and granitoid magma can generate andesitic magma; however, the mixing has to be vigorous because, for reasons of high viscosity related to highly polymerized silicate chains, granitoid magma does not readily mix, as shown by the common presence of mafic “blobs” (also called “enclaves”) in granitoid plutons.

Granitoid magma can also form by other processes, such as hydrous melting of the basaltic (eclogitic/amphibolitic) underplate in a convergent margin (e.g., Rapp and Watson, 1995), fractional crystallization, and silicate liquid immiscibility (as has been observed in the case of layered intrusions). Granitoids and rhyolite do occur on ocean islands and island arcs, where continental

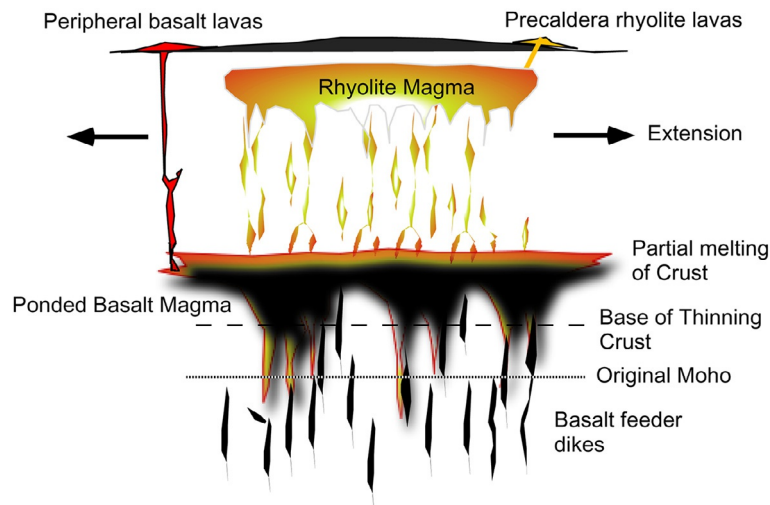


Fig. 17 Melting of the crust by heat released from basalt magma ponded at depth.

crust does not exist, and such magma must be generated by some mechanism involving fractionation of basalt or andesitic magma, remelting of the basaltic underplate, or immiscibility. Andesite magma is unlikely to be primary and its origin is more complicated, as we have seen here. High-Mg andesite primitive magmas ($Mg\# > 65$) with aphyric texture found in some island arcs are likely produced as primary magma in the asthenospheric wedge.

Finally, in seeking primary arc magma compositions, one should remember that all magmas must pass through the mantle wedge and therefore, they must equilibrate with FO_{89-90} olivine. One could thus determine the plausible primary magma compositions by applying an equilibrium Fe/Mg olivine/liquid criterion (as was done by [Leeman et al., 2005](#)). Often the selection is non-trivial and one must filter out obvious olivine or olivine + pyroxene crystal-enriched compositions and calculate potential primary compositions from slightly olivine-fractionated lava compositions. Many authors have used this approach, but here we refer to the exhaustive review of such fractionation-corrected data for worldwide arcs by [Kelemen et al. \(2003\)](#).

[Kelemen et al. \(2003\)](#) found that basalts are more abundant than andesites in the global arc database. In addition to examining the origin of primitive ($Mg\# > 0.6$, as defined by [Kelemen et al., 2003](#)) andesite magmas by mixing between basalt and rhyolite (or granitoid) melts, they also examined two other hypotheses: (1) whether both primitive basalts and andesites are primary magmas formed in the wedge, but the latter simply has greater contribution from subducted sediments \pm mafic crust \pm harzburgite; and (2) whether arc basalts form by greater extent of melting and thus have less slab-derived fluid components. They concluded that both primary basalt and andesite magmas are produced in the wedge; high- $Mg\#$, primitive andesites are likely derived from primary andesite magmas. This is consistent with the more recent findings of [Leeman et al. \(2005, discussed before\)](#). The classic calc-alkaline trend according to [Kelemen et al. \(2003\)](#) is generated from primary andesite magmas.

There are other authors who postulate that andesites are derived from high-alumina basalt (HAB) magmas, and that HABs are primary magmas generated from the mantle in the presence of H_2O . However, others contend that HABs are nothing but andesite magmas that have accumulated an excess of plagioclase phenocrysts perhaps by flotation in magma chambers.

Two important elements of the "arc conversation" that are missing in the above discussion are the physical (i.e., how solids and melts flow in the mantle wedge) and chemical (i.e., phase equilibrium thermodynamics and chemical kinetics at the slab/wedge interface and within the wedge) processes involved in arc magma generation. These are complex issues and we do not yet understand how materials from the subduction zone arrive at the region of melt generation, whether by melt percolation or by diapiric upwelling of slab-top materials and subducted sediment melts and fluids. Discussing these things at length is beyond the scope of this article, and instead we look toward experimental petrologic constraints outlined below.

Fluid-Fluxed Melting in the Asthenospheric Wedge: Insights From Experimental Petrology

Fluid-fluxed melting of the mantle wedge can be triggered in two ways—fluids coming off the descending slab, inducing melting in the wedge above by lowering the solidus temperature so partial melts form; or fluid-rich low-degree melts (from the slab itself or produced closer to the slab) that rise and inflict large-scale melting in the hotter wedge above (e.g., [Kelemen et al., 2003](#)). Here we will not distinguish between the two mechanisms and instead simply examine whether primary high- Mg andesite magma—potentially parent to the global calc-alkaline trend, can be generated from hydrous mantle peridotite. We will focus on a few experiments that provide an insight into how fluids are generated from the descending slab, and to the composition of magmas generated by fluid-fluxed melting from the asthenospheric wedge at pressures of about 3–4 GPa, i.e., over a depth of 90–120 km, above subduction zones.

Fluid Production

Many research groups have examined the P-T conditions where different hydrous minerals in the subducted basaltic (hydrated and altered) crust, sediments, and lithosphere decompose and release fluids. Briefly, these experiments suggest that Mg-rich chlorite, amphibole (in altered basalt), and serpentine (in altered basaltic crust and peridotite in the slab) are the likely hydrous minerals that break down to yield fluids.

Fig. 18 shows the results of three different studies (Kawamoto and Holloway, 1997; Ulmer, 2001; Till et al., 2012) for the peridotite+H₂O system. Also shown is a range of possible dT/dP gradients at the slab/wedge interface (from Grove et al., 2012). Agreement between experiments is good for the stability limits of chlorite and serpentine but not good for amphibole. Till et al. (2012) put the maximum pressure of amphibole stability at less than 2 GPa, whereas Kawamoto and Holloway (1997) put it at about 3.3 GPa. Green et al. (2010) also put it at about 3.2 GPa. Therefore, whether or not amphibole will break down to produce the fluid needed for flux melting of the mantle wedge is debatable, given the dT/dP gradients at the slab/wedge interface shown. On the other hand, it is very likely that chlorite and serpentine breakdown reactions in the slab provide significant fluids to the zone of magma generation.

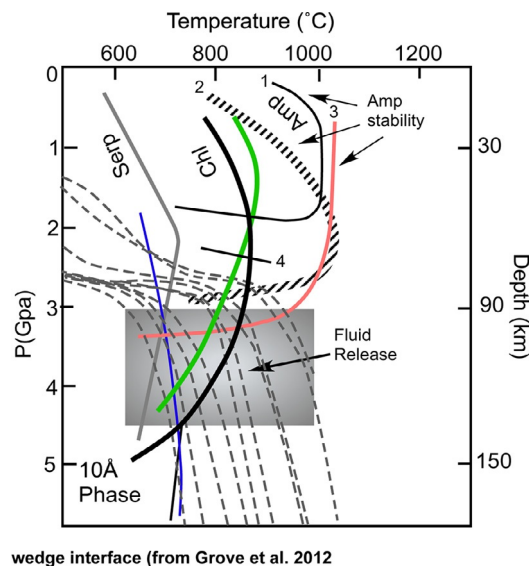
What kind of fluids might these be? Mibe et al. (2007) found that the fluid at about 3.8 GPa is a supercritical fluid in the peridotite-H₂O system. In an isobaric phase diagram, such a supercritical fluid occurs above the second critical point, i.e., the peak temperature on a liquid-vapor immiscibility curve. In the case of subduction, it is likely that supercritical fluid produced from the slab splits into melt and hydrous fluid phases as it rises into the hotter part of the wedge.

Melting and Melt Composition

Melting can only occur when the solidus temperature is exceeded; therefore, it is important to determine the solidi of both hydrous mantle wedge and subducted sediments and altered oceanic crust, preferably at about 3–5 GPa, the pressure of the slab that lies deeper than where mantle wedge melting occurs.

Fig. 19 shows that there is a large discrepancy between different experimental studies about the location of H₂O-saturated lherzolite solidus. For cooler to average temperature gradients (dT/dP) of the slab/wedge interface, the top of the chlorite-bearing slab will begin to melt if Till et al.'s (2012) solidus is correct; and on the other hand, excluding very warm slabs, "normal" slabs will not generally melt if the higher solidi are correct. In this diagram a possible fluid path is shown: fluids will move into the hotter region and thus eventually cross the hydrous wedge peridotite solidus, and thus produce fluid-fluxed magma.

What kinds of melts are generated by fluid-fluxed melting at 3–4 GPa? Conducting high-pressure, high-temperature experiments is very difficult. The studies by Kawamoto and Holloway (1997) and Tenner et al. (2012) suggest that in the presence of H₂O, magmas are alkalic (i.e., nepheline-normative) when forming from a garnet peridotite, which is stable at >2.8 GPa (>100 km deep in the Earth). On the other hand, the magmas are more high-Mg andesitic when they are generated from low to moderate degrees of partial melting of spinel peridotite, shallower in the mantle (e.g., Tenner et al., 2012). Grove et al. (2012) tried to explain the composition of hydrous magmas produced in the mantle wedge (Fig. 20). They suggested that a variety of magmas are generated within the wedge with a fairly constant FeO*/MgO ratio of 0.5–0.8; and the higher-silica versus lower-silica melts are extracted from



wedge interface (from Grove et al. 2012)

Fig. 18 Comparison of stabilities of hydrous phases. Chlorite (Chl), serpentine (Serp) are from Till et al. (2012). Amphibole stability: 1—Till et al. (2012), 2—Ulmer (2001), 3—Kawamoto and Holloway (1997), 4—Fumagalli and Poli (2005). The dashed curves are $\Delta T/\Delta P$ curves at slab-wedge interface. From Grove TL, Till B, and Krawczynski MJ (2012) The role of H₂O in subduction zone magmatism. *Annual Review of Earth and Planetary Sciences* 40: 413–439.

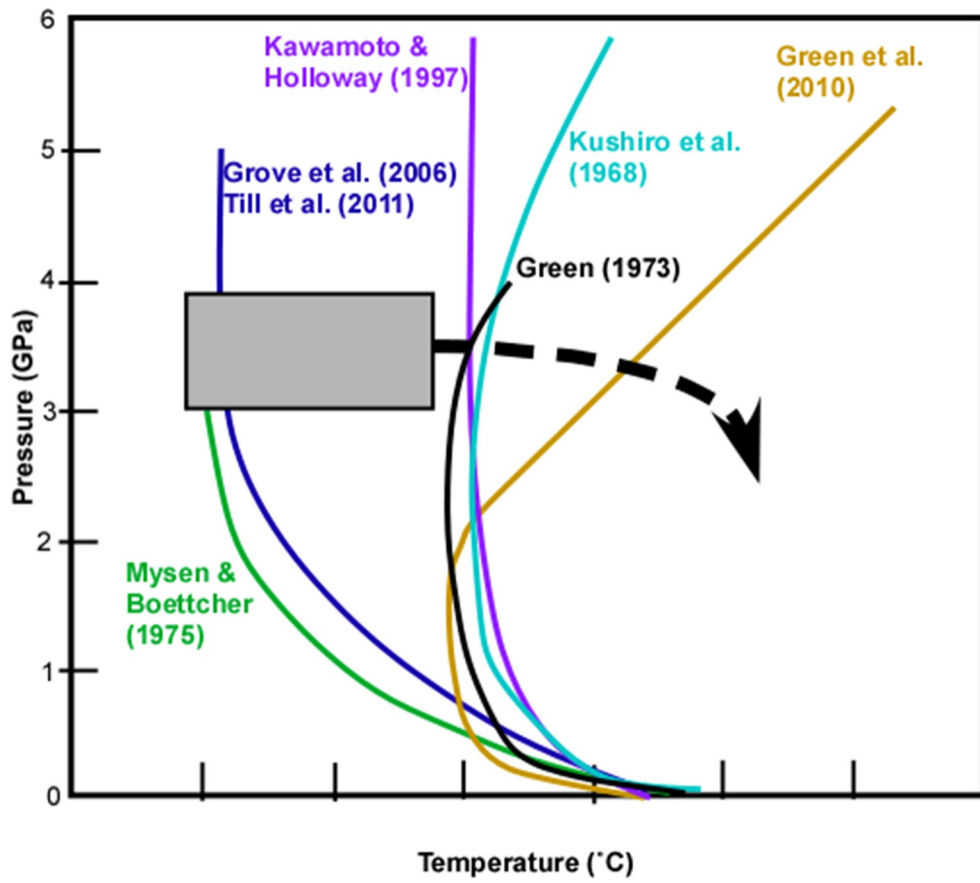


Fig. 19 Solidus of H₂O-saturated lherzolite (fertile mantle) from different studies. The gray box represents possible P-T range of fluid generation from the slab; and black curve represents migration path of the fluids into the hotter part of the wedge. From Grove TL, Till B, and Krawczynski MJ (2012) The role of H₂O in subduction zone magmatism. *Annual Review of Earth and Planetary Sciences* 40: 413–439.

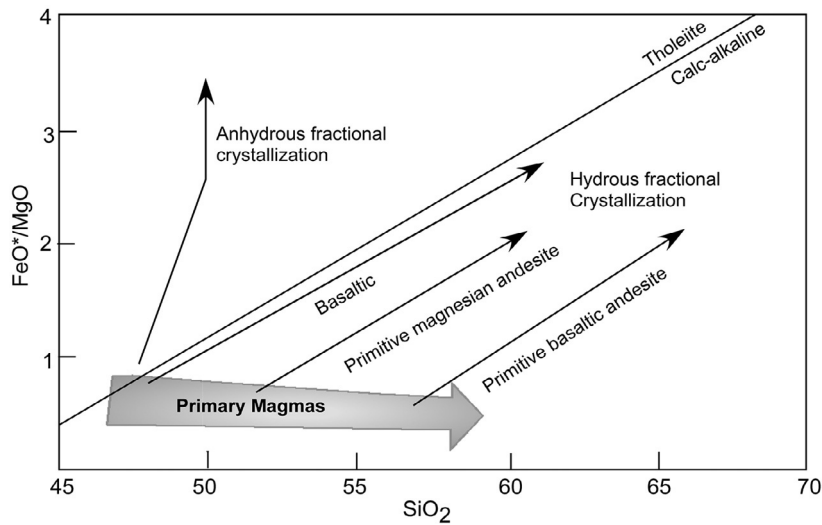


Fig. 20 Primary magmas and fractionation trends in subduction zones. From Grove TL, Till B, and Krawczynski MJ (2012) The role of H₂O in subduction zone magmatism. *Annual Review of Earth and Planetary Sciences* 40: 413–439.

harzburgite vs. lherzolite residues, respectively. Hydrous fractional crystallization produces the calc-alkaline trends. On the other hand, “dry” fractionation of basalt magma generates Fe-enrichment fractionation trends with only a modest increase in silica content.

Johnson and Plank (1999a,b) performed experiments on a pelagic red clay (similar to subducted sediment) at 2–4 GPa in the presence of H₂O. The melts were peraluminous to peralkaline granites, quite different from the lavas erupted at arcs. It is possible that hydrous sediment-derived melts rise from the subducted plate up to the hottest part of the wedge and induce large-scale melting; and this latter (second stage but volumetrically more abundant) melt may be high-Mg andesite.

Summary of Experimental Petrology Results

Magma generation in the asthenospheric wedge above a subducted plate may result from both anhydrous decompression melting as well as by fluid-fluxed melting. While the former process produces tholeiitic basalt magma, the latter process produces a variety of magmas—from alkali basalt to high-Mg andesite. The fluids are generated mostly from chlorite breakdown reaction. Serpentine breakdown may be involved in cooler slabs, but amphibole breakdown as a source of fluid is still debatable. The fluid released may be a supercritical fluid or a fluid+melt composite that rises up to the hotter part of the asthenospheric wedge, where it triggers more voluminous magma generation. Hydrous melting of silicic sedimentary and basaltic rocks in the subducted oceanic crust can also generate small volume granitic melts. Silicic magmas forming large plutons in continental arcs are largely a result of melting of the crust by heat released from a stagnant basalt magma underplate.

References

- Bachmann O and Bergantz GW (2004) On the origin of crystal-poor rhyolites: Extracted from batholithic crystal mushes. *Journal of Petrology* 45: 1565–1582.
- Bailey RA (2004) *Eruptive history and chemical evolution of the precaldera and postcaldera basaltic-dacite sequences, Long Valley, California: Implications for magma sources, current magmatic unrest, and future volcanism*. U.S. Geological Survey. Professional Paper 1692, 76 p.
- Bateman PC and Chappell BW (1979) Crystallization, fractionation, and solidification of the tuolumne intrusive series, Yosemite National Park, California. *Geological Society of America Bulletin* 90: 465–482.
- Clarke DB (1992) *Granitoid Rocks*. London: Chapman and Hall. 283 p.
- Ducea M (2001) The California arc: Thick granitic batholiths, eclogitic residues, lithosphere-scale thrusting, and magmatic flare-ups. *Geological Society of America Today* 11: 4–10.
- Fumagalli P and Poli S (2005) Experimentally determined phase relations in hydrous peridotites to 6.5 GPa and their consequences on the dynamics of subduction zones. *Journal of Petrology* 46: 555–578.
- Green DH, Hibberson WO, Kovačs I, and Rosenthal A (2010) Water and its influence on the lithosphere-asthenosphere boundary. *Nature* 467: 448–451.
- Grove TL and Donnelly-Nolan J (1986) The evolution of young silicic lavas at Medicine Lake Volcano, California: Implications for the origin of compositional gaps in calc-alkaline lava series. *Contributions to Mineralogy and Petrology* 92: 281–302.
- Grove TL, Till B, and Krawczynski MJ (2012) The role of H₂O in subduction zone magmatism. *Annual Review of Earth and Planetary Sciences* 40: 413–439.
- Hildreth W and Wilson CJN (2007) Compositional zoning of the bishop tuff. *Journal of Petrology* 48: 951–999.
- Johnson MC and Plank T (1999a) Dehydration and melting experiments constrain the fate of subducted sediments. *Geochemistry, Geophysics, Geosystems* 1: 1007. <https://doi.org/10.1029/1999GC000014>.
- Johnson MC and Plank T (1999b) Dehydration and melting experiments constrain the fate of subducted sediment. *Geochemistry, Geophysics, Geosystems* 1: 1007. <https://doi.org/10.1029/1999GC000014>.
- Kawamoto T and Holloway J (1997) Melting temperature and partial melt chemistry of H₂O-saturated mantle peridotite to 11 gigapascals. *Science* 276: 240–243.
- Kelemen PB, Yogodzinski GM, and Scholl DW (2003) In: Eiler J (ed.) *Along-strike Variation in Lavas of the Aleutian Island Arc: Implications for the Genesis of High Mg# Andesite and the Continental Crust*. *Geophys. Monogr. Ser.* Washington, DC: AGU.
- Lee C-TA, Cheng X, and Horodyskyj U (2006) The development and refinement of continental arcs by primary basaltic magmatism, garnet pyroxenite accumulation, basaltic recharge and delamination: Insights from the Sierra Nevada, California. *Contributions to Mineralogy and Petrology* 151: 222–242.
- Leeman WP, Lewis JF, Everts RC, Conrey RM, and Streck MJ (2005) Petrologic constraints on the thermal structure of the Cascades arc. *Journal of Volcanology and Geothermal Research* 140: 67–105.
- Mibe K, et al. (2007) Second critical endpoint in the peridotite-H₂O system. *Journal of Geophysical Research* 112: B03201. <https://doi.org/10.1029/2005JB004125>.
- Pitcher WS (1993) *The Nature and Origin of Granite*. London: Blackie Academic & Professional. 321 p.
- Rapp RP and Watson EB (1995) Dehydration melting of metabasalt at 8–32 kbar: Implications for continental growth and crust-mantle recycling. *Journal of Petrology* 36: 891–931.
- Reubi O and Blundy J (2009) A dearth of intermediate melts at subduction zone volcanoes and the petrogenesis of arc andesites. *Nature* 461: 1269–1273.
- Saleeby J, Ducea M, and Clemens-Knott D (2003) Production and loss of high-density batholithic root, southern Sierra Nevada, California. *Tectonics* 22: 1064. <https://doi.org/10.1029/2002TC001374>.
- Stern RJ (2002) Subduction zones. *Reviews of Geophysics* 40. <https://doi.org/10.1029/2001RG000108>.
- Stern RJ, Scholl D, and Fryer G (2016) Convergent plate margin hazards. Plate tectonics and natural hazards. In: Duarte J and Schellart W (eds.) *Plate Boundaries and Natural Hazards*. *Geophysical Monograph* 219, pp. 77–98. AGU.
- Tenner TJ, Hirschmann MM, and Humayun M (2012) The effect of H₂O on partial melting of garnet peridotite at 3.5 GPa. *Geochemistry, Geophysics, Geosystems* 13: Q03016. <https://doi.org/10.1029/2011GC003942>.
- Till CB, Gove TL, and Withers AC (2012) The beginnings of hydrous mantle: Wedge melting. *Contributions to Mineralogy and Petrology* 163: 669–688.
- Ulmer P (2001) Partial melting in the mantle wedge—The role of H₂O in the genesis of mantle-derived ‘arc-related’ magmas. *Physics of the Earth and Planetary Interiors* 127: 215–232.